Functional MRI Signal Changes in Primary Visual Cortex Corresponding to the Central Normal Visual Field of Patients with Primary Open-Angle Glaucoma

Guoping Qing,[1,2] *Shaodan Zhang,*[1,2] *Bo Wang,*[3] *and Ningli Wang*[1]

Purpose. To investigate, by functional magnetic resonance imaging (fMRI), the impact of glaucomatous neuropathy of primary open-angle glaucoma (POAG) on neuronal activity in the primary visual cortex, which corresponds to the central normal visual field.

Methods. Six POAG patients with asymmetric visual field damage and spared central vision were enrolled in the study. All patients underwent detailed ophthalmic examinations, including visual acuity, intraocular pressure, refraction, gonioscopy, and fundus examination. Scanning laser polarimetry with variable corneal compensation, confocal scanning laser ophthalmoscopy, posterior segment optical coherence tomography (OCT), and SITA-standard 30-2 and 10-2 visual field perimetry were also performed on each patient. Block-design fMRI was then performed. The stimulus was a hemifield checkerboard contrast, reversing at 8 Hz and viewed by the examined eye monocularly during fMRI scanning, with the fellow eye occluded.

Results. The blood oxygen level–dependent (BOLD) fMRI signal change in the primary visual cortex corresponding to central visual input from the more severely affected eye was less than that of the fellow eye. Such a difference in fMRI response did not correlate with interocular differences in measurements of scanning laser polarimetry, OCT, and scanning laser ophthalmoscopy, but showed a negative correlation with interocular pattern SD (PSD) difference of visual field analysis.

Conclusions. Glaucomatous neuropathy from POAG may lead to decreased cortical activity in the primary visual cortex, which corresponds to the central normal visual field. The resultant cortical depression is not related to interocular differences in results of polarimetry, OCT, and ophthalmoscopy, but is negatively correlated with PSD of visual field analysis. (*Invest Ophthalmol Vis Sci.* 2010;51:4627–4634) DOI:10.1167/iovs.09-4834

From the [1]Beijing Tongren Eye Center, Beijing Tongren Hospital, Capital Medical University, Beijing Ophthalmology and Visual Sciences Key Laboratory, Beijing, China; and the [3]State Key Laboratory of Brain and Cognitive Science, Institute of Biophysics, Chinese Academy of Sciences, Beijing, China.

[2]These authors contributed equally to the work presented here and should therefore be regarded as equivalent authors.

Supported by a Beijing Municipal Science and Technology Commission grant (Beijing Nova Project 2009BG-01), Ministry of Science and Technology of China Grant 2005CB522800, National Nature Science Foundation of China Grants 30621004 and 90820307, and the Knowledge Innovation Program of the Chinese Academy of Sciences.

Submitted for publication October 28, 2009; revised December 4, 2009, and February 24, 2010; accepted March 16, 2010.

Disclosure: **G. Qing**, None; **S. Zhang**, None; **B. Wang**, None; **N. Wang**, None

Corresponding author: Ningli Wang No. 1, Dongjiaominxiang, Dongcheng District, Beijing, 100730, China; wningli@vip.163.com.

Glaucoma is one of the leading causes of irreversible blindness worldwide. It is projected to affect 61 million people worldwide by 2010.[1] Progressive retinal ganglion cell (RGC) loss and the resultant visual field defect are the hallmarks of glaucoma. Among all clinical types of glaucoma, primary open-angle glaucoma (POAG) is one of the most common in all ethnic groups and is most prevalent in adults, particularly elderly people. The course and progression of POAG is usually asymptomatic. Extramacular regions are the first to deteriorate, and thus before those affected notice any problem, they may have severe visual disability. That is one of the main reasons why POAG causes a high rate of blindness.

The visual field defect characteristic of POAG usually but not always begins from the midperipheral regions, like a nasal step defect or paracentral scotoma.[2–4] In some advanced cases, central vision can be well preserved until the very late stage of the disease, leading to tunnel vision.[5] Although the central vision may remain normal, the patients' quality of life is affected, however, because of both the constricted visual field and the impaired detection of global motion, global form integration, color perception, and/or contrast sensitivity of the residual vision.[6–11] It has also been suggested that patients with glaucomatous field defect may find more difficulties with complicated visual tasks than is predicted through their field defect.[12] Decreased neuronal cell density and biological activity in the visual pathway and/or primary visual cortex have been demonstrated in both glaucoma animal models and patients.[12,13] In these studies, several methods, such as visual evoked potentials (mfVEPs), positron emission tomography (PET), and single-photon–emission computed tomography (SPECT) have been used to measure the functional alterations in glaucomatous neuropathy resultant from central neural activity in vivo.[14–21] Based on the fact that RGCs of the macula and paracentral retina project to different parts and layers of the visual cortex, the structural and functional changes in cortical neurons corresponding to midperipheral and peripheral fields could be modified in POAG. However, the mentioned investigative techniques are restricted by either poor spatial resolution or the requirement for radioisotopes, and no powerful evidence is available so far regarding the functional status of the primary visual cortex that corresponds to central normal vision. High-resolution functional magnetic resonance imaging (fMRI), which is based on the blood oxygen level–dependent (BOLD) contrast technique, provides us an ideal choice because it possesses the advantages of high spatial resolution, noninvasiveness, and the ability to reflect task-related neuronal activity.[22,23] Previous studies have demonstrated that the spatial pattern of fMRI response observed in V1 is in agreement with the pattern of visual field loss measured by automated perimetry (in a retinotopic fashion).[24,25] This outstanding retinotopic localization ability of fMRI allows it to be a suitable method for physiopathological research in the visual pathway. In the present study, we attempted to use fMRI to

Copyright © Association for Research in Vision and Ophthalmology

Downloaded from iovs.arvojournals.org on 01/17/2022

test the hypothesis that the primary visual cortex corresponding to the central, apparently normal visual fields may be affected in POAG patients. Should the status of the cortex be found to be altered, then it may not only help us to better understand the pathophysiological characteristics of the disease but may also lead to new neuroprotective strategies in glaucoma treatment.

METHODS

Subjects

Six POAG patients (four women and two men; mean age, 49.5 years) with asymmetric visual field damage were enrolled in the study. The subjects were examined in Beijing Tongren Eye Center, Capital Medical University. By contrast to the glaucomatous eye, the fellow eye was either unaffected or less affected, as shown by automated perimetry. Central vision was preserved in both eyes. The follow eye served as a control to minimize the variability among patients. All subjects underwent a thorough ophthalmic examination, including visual acuity, refraction, intraocular pressure (IOP) measurement, undilated and dilated slit lamp examination, gonioscopy, direct ophthalmoscopy, and nonmydriatic retinal photography. Visual fields were assessed using standard automated perimetry (Humphrey 30-2 and 10-2 SITA program; Carl Zeiss Meditec, Dublin, CA).

Scanning laser polarimetry with variable corneal compensation (GDx-VCC; Carl Zeiss Meditec) and confocal scanning laser ophthalmoscopy (Heidelberg Retina Tomograph II [HRT-II]; Heidelberg Engineering, Heidelberg, Germany) were used to measure retinal nerve fiber layer (RNFL) thickness and optic disc topography, respectively. Fourier-domain optical coherence tomography (RTVue-100; Optovue, Inc., Fremont, CA) was used to access macular thickness. The macular thickness map, which represented approximately the central 20° of vision, was divided into nine sections, displayed as three concentric circles, including a central circle, an inner ring, and an outer ring, with each ring divided into four quadrants. The central circle, inner ring, and outer ring had diameters of 1, 3, and 6 mm, respectively. Retinal thickness maps were color coded, with brighter colors for thicker retinal areas and darker colors for thinner ones. Retinal thickness of each section was labeled.

Test images and photographs were evaluated for quality and reliability. Detailed information on the subjects is shown in Table 1. Excerpts from GDx-VCC, OCT, HRT-II, and visual field perimetry printouts of an example subject are also displayed (Fig. 1).

All patients were right-handed and had a best corrected visual acuity of 20/40 or better. The difference in refraction between the eyes within a patient was equal to or less than 2.5 D. An uncomplicated laser treatment or glaucoma surgery was included in our series. Among the enrolled subjects, patient 2 underwent nonpenetrating trabecular surgery (NPTS) on her right eye for uncontrolled IOP. She had undergone selective laser trabeculoplasty in both eyes 1 year earlier, but the IOP in the right eye was still uncontrolled after the laser treatment. The other five patients were receiving topical antiglaucoma medications, with no history of laser treatment or antiglaucoma surgery.

Eyes that exhibited signs of nonglaucomatous retinal disease (like optic neuritis, retinitis pigmentosa, and diabetic retinopathy), opaque media, or other ocular diseases that could affect the visual field (such as retinal vascular diseases and ocular tumors) were excluded. Subjects with contraindications to MRI scanning were also excluded, which included being fitted with a pacemaker or other metal in the body, history of claustrophobia or other psychological disorder, weak general condition, and pregnancy.

We certify that our research adhered to the tenets of the Declaration of Helsinki. All applicable institutional and governmental regulations concerning the ethical use of human subjects were complied with during this research. Informed consent was obtained from all subjects.

fMRI Methodology: Visual Stimuli and Data Acquisition

Visual stimuli consisted of black-and-white checkerboards with contrasting components that reversed at 8 Hz. Each experimental run lasted 400 seconds, which was divided into eight epochs of 50 seconds' duration. Each epoch contained a 30-second checkerboard stimulus (task phase or on-phase) and a 20-second unpatterned background with the same mean luminance as the stimulus period (baseline phase or off-phase). During the task phase, either a 24° × 36° full-screen checkerboard or a 5° sectoral checkerboard (180°) was randomly presented on the screen, four times for each phase. The full-screen

TABLE 1. Basic Information of Enrolled Patients

						HFA				HRT-II		GDx-VCC		OCT	
						30-2		10-2							
Subject	Age (y)	Sex	Eye*	IOP (mm Hg)	More Affected Hemifield†	MD	PSD	MD	PSD	MRNFL (mm)	CDR	TSNIT Average (μm)	S/I Average‡ (μm)	Central Ring (μm)	Inner Ring§ (μm)
1	45	F	OSg	20.5	S	−16.22	15.10	−13.03	13.54	0.126	0.687	31.5	37.2	238	301
			ODf	17.3	S	−9.12	11.35	−4.54	6.53	0.133	0.659	35.5	39.7	243	306
2	55	F	ODg	25	S	−9.86	13.08	+0.15	1.87	0.25	0.477	33.0	38.8	277	306
			OSf	30	Normal	+1.04	2.13	+0.57	0.88	0.343	0.380	49.7	62	275	308
3	22	F	OSg	24	I	−14.42	13.86	−7.21	7.45	0.166	0.650	25.4	38.8	291	315
			ODf	24.5	I	−8.78	7.95	−4.31	2.21	0.186	0.747	30.7	43.5	239	300
4	30	F	OSg	29	S	−8.60	11.56	−2.90	2.72	0.439	0.214	44.0	66.4	220	307
			ODf	28	Normal	−2.08	3.29	−1.60	0.88	0.209	0.341	47.8	60.2	215	303
5	76	M	ODg	33	S	−10.73	15.12	−14.27	15.68	0.170	0.435	42.5	58.9	234	295
			OSf	31	Normal	−0.69	1.64	−1.01	1.18	0.113	0.454	42.9	59.8	235	291
6	69	M	ODg	17	S	−16.86	13.12	−5.05	5.68	0.138	0.734	33.5	34.7	270	296
			OSf	18	Normal	−1.92	3.86	−3.06	1.01	0.266	0.523	40.2	48.3	257	300

CDR, cup-to-disc ratio.

* g, glaucomatous; f, fellow.

† The visual field was divided into two parts: superior (S) and inferior (I) hemifields. The more affected hemifield was defined according to the outcome of HFA 30–2 SITA standard test.

‡ Average nerve fiber thickness in the superior or inferior quadrant corresponding to the less affected visual hemi-field as revealed by GDx-VCC was presented.

§ Retinal nerve fiber thickness of the inner ring in the superior or inferior macular quadrant corresponding to the less affected visual hemifield as revealed by Optovue OCT (Fremont, CA) was presented.

Downloaded from iovs.arvojournals.org on 01/17/2022

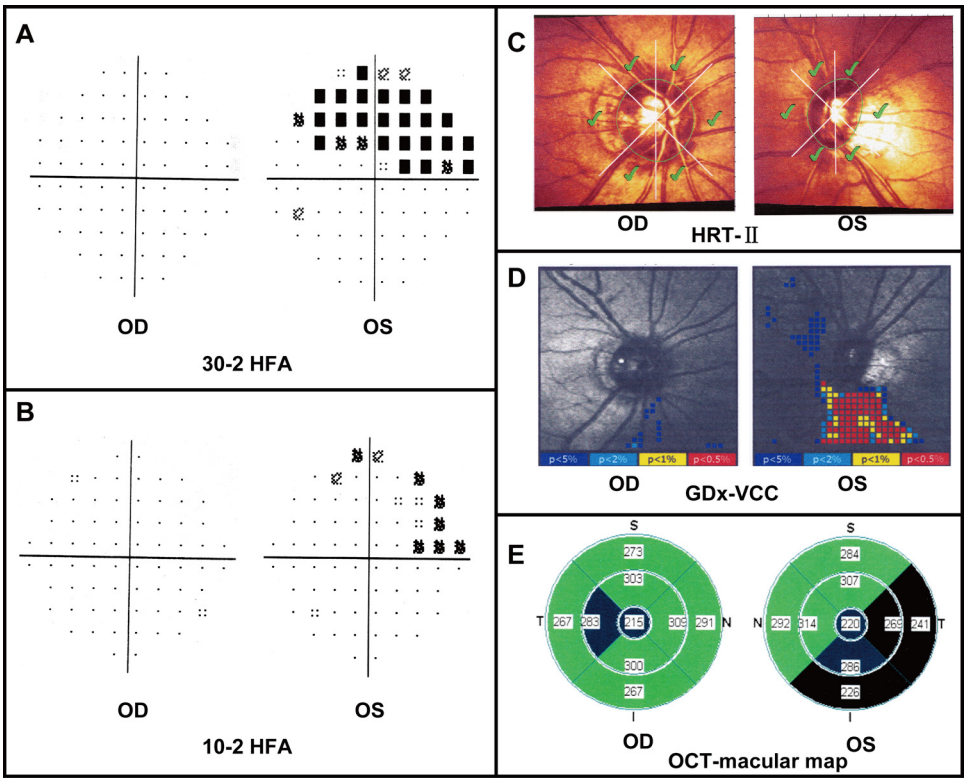

FIGURE 1. Illustrative visual field outcomes and excerpts from retinal structure measurements of a 30-year-old female POAG patent. The 30-2 and 10-2 visual field perimetry programs both revealed a visual field defect in the superior region in the left eye. The right eye was relatively normal (**A**, **B**). Scanning laser polarimetry with variable corneal compensation (GDx-VCC) demonstrated a reduction in RNFL thickness in the inferior quadrant of the left retina, which was consistent with the visual field analysis (**D**). The macular map of the OCT instrument also illustrated RNFL thinning in the inferior retina in the left eye (**E**). No obvious RNFL changes were observed in either eye by scanning laser ophthalmoscopy (HRT-II). *Green check marks* indicate that RNFL thickness for a given sector is within normal limits (**C**).

checkerboard stimulus was designed to test another hypothesis. The data describing the full-screen stimulus will not be discussed here. The central checkerboard stimulus was presented to the less affected upper or lower hemifield according to subjects' visual field outcomes (Fig. 2). The subjects were asked to fix their eyes on the cross presented at the center of the screen during the run. A monocular stimulus was obtained by covering one eye with an occluder attached to the goggle. The glaucomatous eye and the fellow eye were tested alternatively. Refractive error was corrected with lenses fixed on the goggle according to refraction results. The stimuli were generated by a computer and were back projected on a screen that was located inside the MRI bore near the patient's head. Subjects viewed the screen at a total path length of 60 cm through a mirror situated above their eyes.

MRI images were acquired by a 3-Tesla scanner (Trio; Siemens, Erlangen, Germany) in the Beijing MRI Center for Brain Research. The subject was positioned supine in the bore with the head centered in a standard bird-cage quadrature head coil. Head movement was minimized by two pieces of foam surrounding the subject's head. Functional images were acquired with a T_2^*-weighted gradient-echo, echo-planar pulse sequence: 25 axial slices (4-mm thick with a 1-mm gap); echo time (TE), 30 ms; repetition time (TR), 2000 ms; flip angle (FA), 60°; matrix, 64 × 64; in-plane resolution, 3.4 × 3.4 mm^2. For an anatomic reference image, a T_1-weighted MR volume image was acquired, in each fMRI experiment, after the fMRI session with a resolution of 1.0 × 1.0 × 1.3 mm: MP-RAGE, 144 sagittal slices; TE, 3.37 ms; TR, 2560 ms; flip angle, 7°; and matrix, 256 × 256.

Data Analysis

Image processing and statistical analysis were performed with SPM5 (Wellcome Department of Cognitive Neurology, London, UK). The first two volumes of each session were discarded. For each subject, all volumes were spatially realigned to the first volume of the first session to correct head motion, and coregistered to the patient's 3-D anatomic image, which were spatially normalized to Montreal Neurologic Institute (MNI) reference space with a 12-parameter affine normalization and 12 nonlinear iterations with a 7 × 8 × 7-basis function. All volumes were spatially smoothed with a 6-mm full-width-half-maximum (FWHM) isotropic Gaussian kernel. The BOLD signal time series across each voxel was high-pass filtered with an upper cutoff of 128 seconds. Autocorrelations between sessions and epochs were modeled by a standard hemodynamic response function at each voxel.[26]

For regions of interest (ROI) analysis, the time course of signal change was extracted from the individual ROI in each eye of each subject. The average percentage signal change (PSC) was calculated by using the average signal intensity during all unpatterned black-background epochs as a baseline. Because the fMRI response typically lags 4 to 6 seconds after the neural response, our data analysis procedure treated the first two functional images of each epoch as belonging to the condition of the previous epoch and omitted the next two images (during the transition between conditions) from the analysis.

The Kolmogorov-Smirnov test was used to assess whether the data have a normal frequency distribution or not. A paired *t*-test was used to compare the mean PSC values and the number of activated voxels between the fellow and the glaucomatous eyes of each subject. fMRI signal changes in the primary visual cortex were compared to the parameters of visual field analysis and structural measurements of the optic disc/RNFL using correlation analysis. Pearson and Spearman correlation analysis were used for parametric and nonparametric data, respectively. $P < 0.05$ was statistically significant (all statistical analyses: SPSS, ver. 11.5; SPSS, Inc. Chicago, IL).

RESULT

fMRI Responses in the Visual Cortex

The central checkerboard stimuli presented to the monocularly viewing eye evoked a significant BOLD signal increase in the primary visual cortex, especially in the bilateral occipital poles. Figure 3 shows the typical BOLD responses of a POAG patient. Yellowish pixels correspond to voxels where the task-induced BOLD signal was significantly increased compared with that of the baseline (Fig. 3A). The number of activated

Downloaded from iovs.arvojournals.org on 01/17/2022

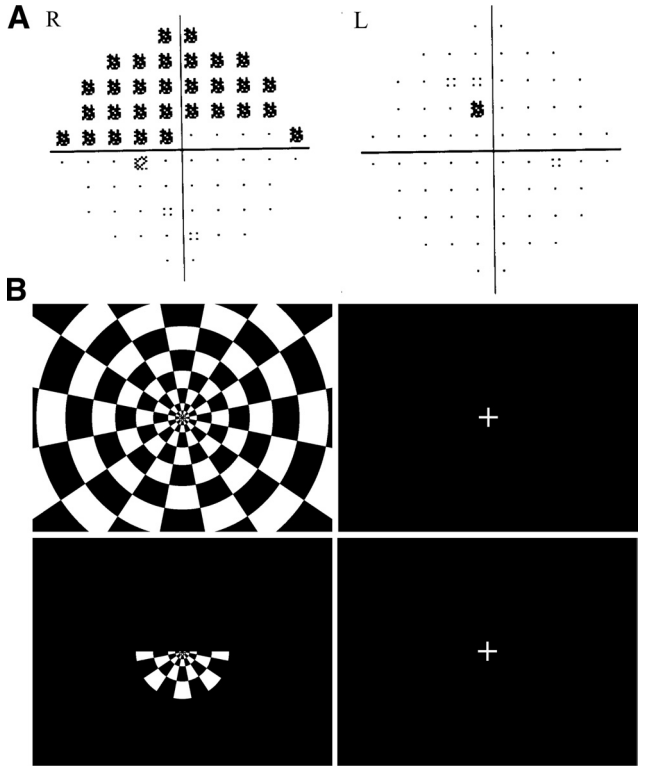

FIGURE 2. Stimuli used in the fMRI scanning. (**A**) Example of a statistical map of the visual field perimeter's 10-2 SITA-standard analysis. A diffused visual field defect was detected in the superior hemifield of the right eye. The left eye was relatively normal. (**B**) Each run consisted of a 30-second checkerboard stimulus (task phase) and a 20-second rest (baseline phase). In the baseline condition, a cross appeared at the center of the black background. In the task phase, either a full-screen or a central checkerboard randomized by the computer was presented. The central checkerboard reversing at 8 Hz was projected to the less affected hemifield, according to the outcomes of visual field perimetry. In this patient, the central visual stimulus was set to the inferior hemifield.

voxels elicited by viewing through the glaucomatous eye (2086 ± 1063; 95% confidence interval [CI], 970–3201) did not differ from that elicited by viewing with the fellow eye (1813 ± 1239; 95% CI, 513–3112; $P = 0.428$; Figs. 3B, 3C).

fMRI responses to the checkerboard stimuli were expressed as the percentage change of BOLD amplitude between the task-induced and the baseline-induced BOLD signals. The mean percentage of BOLD signal change of each eye was averaged over four scans for each subject. Viewing with the glaucomatous eye consistently elicited a less prominent BOLD signal change in the primary visual cortex than viewing with the fellow eye in all POAG patients (Fig. 4). When fMRI BOLD mean percentage signal changes were averaged across subjects for the fellow and the glaucomatous eyes, respectively, a significant decrease in the glaucomatous eye–evoked BOLD signal change (1.539 ± 0.165; 95% CI, 1.366–1.712) was observed in comparison with that in the fellow eye (1.752 ± 0.204; 95% CI, 1.538–1.967; $P = 0.004$; Fig. 4B). The time courses of BOLD signal change in the fellow and the glaucomatous eyes were investigated by using the mean value of each scan averaged over the six patients (Fig. 5). The BOLD response pattern was similar between the fellow and glaucomatous eyes. However, when viewing the checkerboard stimulus, the fellow eyes elicited a sharper BOLD response than did the glaucomatous eyes.

RNFL Thickness in the Macular Region Measured by OCT

Excerpts from the macular map (EMM5) retina report of the OCT system (RTVue-100; Optovue) for a typical patient are presented in Figure 1E. We compared the bilateral retinal thickness in the central circle and the inner ring in the quadrant corresponding to the less affected hemifield in each patient. Statistical analysis demonstrated that there was no difference in macular thickness between the glaucomatous and the fellow eyes in these two regions ($P = 0.47$ and 0.68, respectively).

Correlations between fMRI Responses and Visual Field or Retinal Structural Parameters

BOLD responses to the central checkerboard stimuli were compared to the parameters of visual field analysis and structural measurements of the optic disc/retinal nerve fiber layer (RNFL). Difference scores for BOLD responses (BOLD-DIF) elicited by binocular eyes in each subject were calculated by subtracting the corresponding values related to the glaucomatous eye from that of the fellow eye. It was compared with the interocular difference in parameters of visual field analysis, which involved MD and PSD of both 30-2 and 10-2 SITA standard strategies (referred as MD30-DIF, PSD30-DIF, MD10-DIF, and PSD10-DIF). The absolute values of these scores were used to do the correlation analysis. Among these parameters, only PSD30-DIF score demonstrated a borderline significant correlation with BOLD-DIF ($r = -0.811$, $P = 0.050$). The larger the interocular difference in visual field defects as revealed by PSD30-DIF, the smaller the BOLD-DIF (Fig. 6). Difference scores for mean RNFL thickness or RNFL thickness in the quadrant corresponding to the stimulated visual field measured by scanning laser polarimetry, scanning laser ophthalmoscopy, and OCT were also calculated. No significant correlation was found between these retinal structural measurements and the BOLD-DIF.

DISCUSSION

In this study, we measured the cortical response to visual stimuli presented to the apparently normal central visual field in patients with asymmetric POAG. The fellow eye served as a control to minimize the variability among patients. Despite the small sample size, a consistent trend was noted in each subject. Compared with the fellow eyes, the glaucomatous eyes showed a decreased BOLD response in the primary visual cortex. Consistent with previous studies, it suggests that even in the visual field defined as the normal central area, there may be a functional decrease in POAG patients.[9–15] These patients may have greater difficulties in dealing with their daily visual tasks than are predicted by their visual field loss.[12]

Task-Related BOLD Response Decrease in the Primary Visual Cortex

The decreased cortical BOLD response evoked by the glaucomatous eye may be due either to a flow-on effect of early perceptual loss or to cortical abnormalities.[27–31]

Since the visual acuity is well kept until the late stage of glaucoma, it is generally believed that the papillomacular bundle is relatively resistant to the pathologically increased IOP. However, morphologic findings demonstrated that the thickness of the papillomacular bundle and the macular are both decreased in glaucomatous eyes with good visual acuity.[32–34] In the present study, we measured the macular thickness by Fourier-domain OCT (RTVue-100; Optovue). Consistent with previous studies, the macular map revealed a thickness de-

Downloaded from iovs.arvojournals.org on 01/17/2022

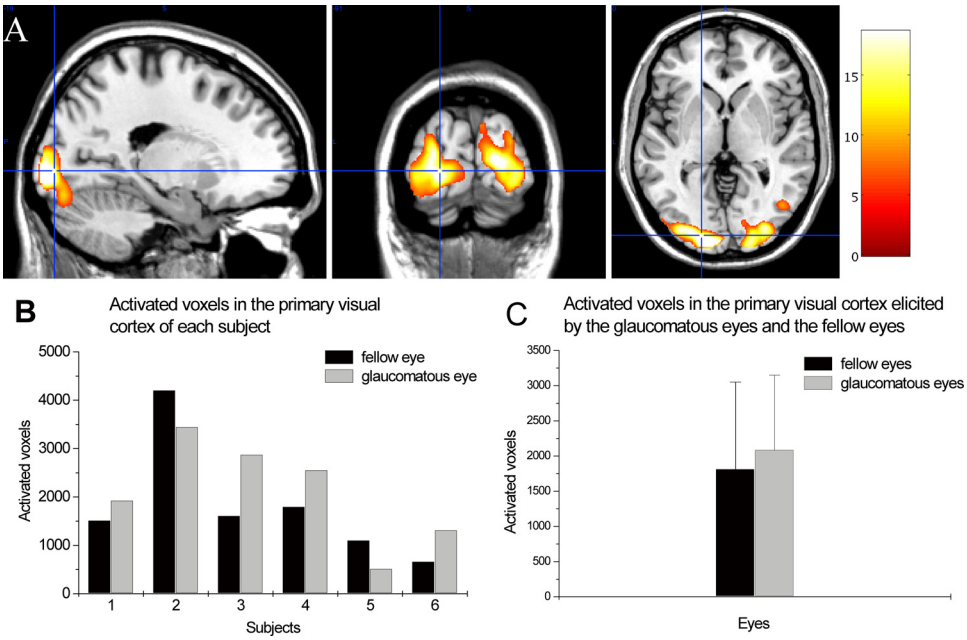

FIGURE 3. Cortical responses to the central visual stimuli in the primary visual cortex. (**A**) A monocular central reversing checkerboard stimulus evoked a significant BOLD response in the bilateral occipital lobes. Representative images are shown of the BOLD response elicited from the glaucomatous eye of a subject. Sagittal, coronal, and axial sections are shown separately. Pseudocolor represents the area of significantly activated voxels. (**B**) The number of activated voxels in the primary visual cortex elicited by the glaucomatous eye and the fellow eye are shown for each patient. (**C**) Activated voxels for the glaucomatous eyes and the fellow eyes were averaged over individual patients. The number of glaucomatous eye–activated voxels in the visual cortex did not differ from the number activated by the fellow eye (2086 ± 1063 in the glaucomatous eyes vs. 1813 ± 1239 in the fellow eyes; $P = 0.428$).

crease in our series. To evaluate the perceptual difference between bilateral eyes, we investigated the macular thickness in the quadrant corresponding to the stimulated central visual field in all enrolled patients. Statistical analysis demonstrated that there was no difference in the macular thickness in these specific areas between the glaucomatous eye and the fellow eye. Although this result provides structural evidence, we still cannot draw a strong conclusion that the retinal input is equal in bilateral eyes. A substantial number of RGCs have already died before obvious visual field defects can be detected.[35] At least 25% to 35% RGC loss occurs before any statistical abnormality in automated visual field testing.[27] In addition to the loss of M-type RGCs in the peripheral retina,[36–38] loss of central ganglion cells has also been observed in eyes with mild glaucomatous damage, suggesting a diffuse RGC damage in the glaucomatous eye before a functional impairment.[28,29] Meanwhile, recent studies have revealed that the somata and dendritic arbors of surviving retinal ganglion cells expand in animal models of glaucoma. This compensatory adaptation leads to a significant increase in central visual receptive-field size across the brain.[39,40] It implies that, in the present study, the 5° visual stimulus presented to the glaucomatous eye may be received and processed by fewer RGCs than the fellow eye. From these points of view, although the central visual field is apparently "normal," the retinal input of this region may have already been reduced, leading to the decrease of activity in the visual cortex.

Postretinal neuropathy may also contribute to the decreased BOLD response in the primary visual cortex. Recently, accumulating evidence supports the hypothesis that glaucomatous neuropathy involves the whole visual pathway. Besides injury to the optic nerve, neurodegeneration in the brain has also been reported in glaucoma. Changes in cell morphology,[41,42] neuronal metabolic activity,[30,31] and the expression pattern of specific proteins in LGN and visual cortex[43] have been observed both in primate glaucoma models and in POAG patients. These changes in brain neurons may lead to functional alterations. In a cat model of retinal photocoagulation, the deafferented contralateral dLGN displayed a decrease in cell size and a concomitant inexcitability to light.[44] Since atrophy of the visual cortex has been reported in patients with severe long-term POAG, it is possible that changes of visual cortex may be related to a compromised excitability and therefore lead to a decreased BOLD response in these patients.

From another point of view, we should note that BOLD as a measure of neural activity relies on the regulation of blood vessels. The decreased BOLD signal observed in our study may also have resulted from a disturbed cerebral vascular activity in POAG patients. Neurons may directly control the local changes in cerebral blood flow (CBF) associated with neuronal activity.[45–47] Neuronal atrophy and loss in the postretinal visual pathway in glaucoma patients may affect the neuron-vascular coupling and lead to a reduced BOLD signal change.[12,30,31,41–43,48–55] Meanwhile, other studies have revealed that glial cells also play a pivotal role in

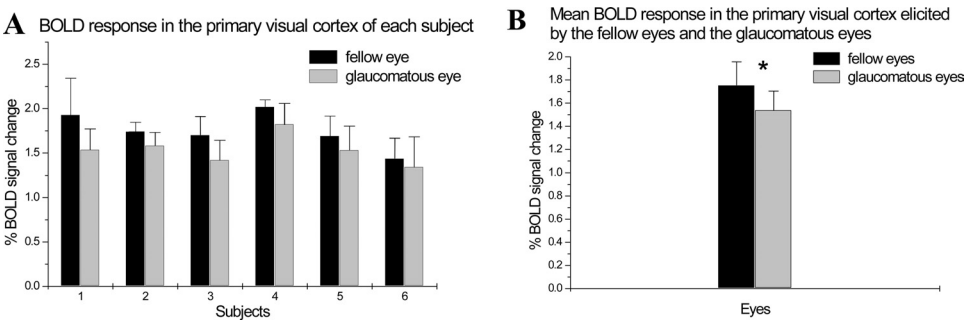

FIGURE 4. BOLD signal changes of the patients. (**A**) Averaged BOLD signal changes over four scans were shown for the glaucomatous eye and the fellow eye in each patient. Histograms represent the mean percentage of BOLD signal change of each eye averaged over four scans for each subject. Standard error bars were also shown. In all patients, viewing through the glaucomatous eye evoked a smaller BOLD response than viewing through the fellow eye. (**B**) Averaged BOLD signal changes over individual patients demonstrated a decreased BOLD response to the central visual stimuli presented to the glaucomatous eye (1.752% ± 0.204% for the fellow eyes vs. 1.539% ± 0.165% for the glaucomatous eye; $^*P = 0.004$).

Downloaded from iovs.arvojournals.org on 01/17/2022

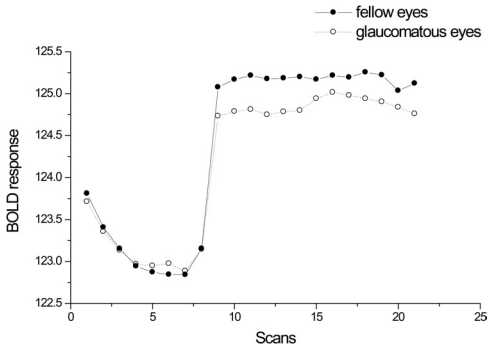

FIGURE 5. This plot represented the mean signal changes over time in the glaucomatous eyes versus the fellow eyes across six patients. Under the condition of baseline, fellow eyes and glaucomatous eyes induced a similar BOLD response in the visual cortex. When receiving checkerboard stimuli, the fellow eyes elicited a much sharper BOLD response than did the glaucomatous eyes and reached a higher amplitude.

neurovascular coupling.[56,57] Local arteriolar dilation in response to high neuronal activity largely depends on the activation of astrocytes (glutamate-mediated $[Ca^{2+}]_i$ oscillations in astrocytes) by locally released vasoactive compounds.[58–60] There is evidence that, in primate glaucoma models, the intensity of astrocytes is much more in the LGN layers that receive a retinal input from the high-IOP eye than in those that receive input from the contralateral untreated eye.[51] This region-specific astrocyte proliferation in the central visual targets may disrupt the astrocyte-mediated regulation of local arterioles and therefore result in a decreased BOLD signal change in the primary visual cortex during visual stimulation. In addition, direct evidence of cerebrovascular insufficiency in glaucoma patients has also been addressed. They may have diffuse cerebral small vessel ischemia and cerebral infarcts.[61,62] Diastolic blood pressure of cerebral vessels is significantly higher in glaucoma patients than in control subjects at baseline and during hyperoxia.[63] There is a significant correlation between the mean flow velocity of middle cerebral arteries (MCAs) and the mean defect of the central visual field, logMAR visual acuity, and contrast sensitivity in glaucoma patients, suggesting that, in certain POAG patients, diminished central visual function may be one manifestation of widespread cerebrovascular insufficiency.[64] In the primary visual cortex, ocular dominance columns driven by the ipsilateral and contralateral eyes may be supplied by a different microvascular system.[65,66] The vascular insufficiency in regions receiving retinal input from the glaucomatous eye is likely to be more severe than that related to the fellow eye, which may affect the task-related blood flow increase during visual stimuli to the glaucomatous eye and lead to a reduced BOLD response.

Correlation between fMRI Responses and Visual Field Analysis or Optic Nerve Fiber/Head Structure Measurements

The most unexpected result of our study is that we find a borderline negative correlation between PSD30-DIF and BOLD-DIF. The more affected the visual field, the less affected the BOLD response. This phenomenon may imply a replasticity or a compensatory mechanism of the visual pathway. On one hand, peripheral scotoma may have a potentiating effect on the central reserved visual field. Surviving retinal axons may compete and compensate for the lost retinal axons and therefore relatively enhance the visual signal input. On the other hand, decreased retina input may result in replasticity of the cortical neurons and enhance the information processing and integrity ability of the visual cortex. Enhancing the compensatory ability of the visual pathway may be an alternative way to improve the visual function of glaucoma patients.

In our study, no correlation was found between BOLD-DIF and the parameters of RNFL measurements, as revealed by GDx, HRT, and OCT. This result is inconsistent with that of Duncan et al.[24] They presented a checkerboard to the visual space with the greatest visual loss and found a cortical activity decrease in POAG patients in a manner consistent with damage to the optic disc. The discrepancy may be due to the different retina regions that were stimulated during scanning. In the defective visual field, most of the RGCs have already died. These regions are likely to have a thinner RNFL and a reduced retinal input. What's more, fMRI scanning measures the output resulting from activation of each successive level of the visual system, whereas GDx, HRT, and OCT only estimate the structure changes at the retina level. All these facts put forward the necessity of developing new methods that can integrate the functional and structural evaluations of the visual pathway better.

Limitations of the Present Study

Glaucoma is usually a bilateral ocular disease. The fellow eye will exhibit visual damage years after that of the first eye affected. Because of the silent progression and binocular compensation, generally, when patients come to the clinics, both eyes are affected. It is difficult to collect POAG patients with extremely asymmetric visual field damage. What's more, some older patients that met our research requirements had contraindications for MRI examination, among which the pacemaker is the most common. These factors ultimately limited the sample size of the present study. Small sample size may bring problems of variability and limited power to draw a conclusion. However, in the present study, a consistent trend of BOLD signal decrease in the primary visual cortex corresponding to the central normal visual field in the glaucomatous eye relative to the fellow eye was noted in all six POAG patients, which encouraged us to believe that it is not a coincidence.

In summary, the present findings led us to the tentative conclusion that POAG patients may have a functional decrease in the apparently normal central visual field. This result shifts our focus from visual fields that are lost to those that are reserved. fMRI may be a promising tool for detecting early glaucoma that is not detected with behavioral measures.

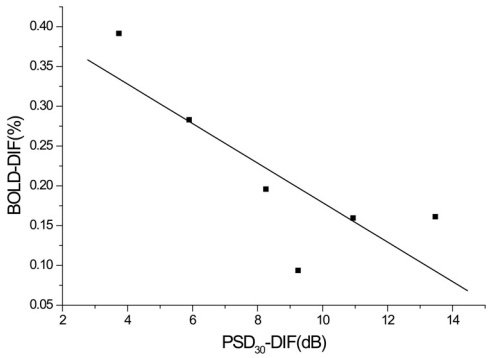

FIGURE 6. The effect of visual field defects on BOLD responses. There was a borderline significant correlation between the difference in scores of BOLD responses (BOLD-DIF) and PSD in 30-2 SITA standard automated perimetry (PSD30-DIF; $r = -0.811$, $P = 0.050$).

Downloaded from iovs.arvojournals.org on 01/17/2022

Acknowledgments

The authors thank Tao Wang and Lan Wang for referring POAG patients for the study, and HuaiZhou Wang, ShuZhen Guo, and Qian Wang for assistance in performing the ophthalmic examinations.

References

1. Quigley HA, Broman AT. The number of people with glaucoma worldwide in 2010 and 2020. *Br J Ophthalmol.* 2006;90:262–267.
2. Werner EB, Beraskow J. Peripheral nasal field defects in glaucoma. *Ophthalmology.* 1979;86:1875–1878.
3. Werner EB, Drance SM. Early visual field disturbances in glaucoma. *Arch Ophthalmol.* 1977;95:1173–1175.
4. Harwerth RS, Smith EL 3rd, DeSantis L. Behavioral perimetry in monkeys. *Invest Ophthalmol Vis Sci.* 1993;34:31–40.
5. Much JW, Liu C, Piltz-Seymour JR. Long-term survival of central visual field in end-stage glaucoma. *Ophthalmology.* 2008;115:1162–1166.
6. Ansari EA, Morgan JE, Snowden RJ. Psychophysical characterisation of early functional loss in glaucoma and ocular hypertension. *Br J Ophthalmol.* 2002;86:1131–1135.
7. McKean-Cowdin R, Wang Y, Wu J, Azen SP, Varma R. Impact of visual field loss on health-related quality of life in glaucoma: the Los Angeles Latino Eye Study. *Ophthalmology.* 2008;115:941–948-e941.
8. McKendrick AM, Badcock DR, Morgan WH. Psychophysical measurement of neural adaptation abnormalities in magnocellular and parvocellular pathways in glaucoma. *Invest Ophthalmol Vis Sci.* 2004;45:1846–1853.
9. McKendrick AM, Badcock DR, Morgan WH. The detection of both global motion and global form is disrupted in glaucoma. *Invest Ophthalmol Vis Sci.* 2005;46:3693–3701.
10. Sampson GP, Badcock DR, Walland MJ, McKendrick AM. Foveal contrast processing of increment and decrement targets is equivalently reduced in glaucoma. *Br J Ophthalmol.* 2008;92:1287–1292.
11. Stamper RL. The effect of glaucoma on central visual function. *Trans Am Ophthalmol Soc.* 1984;82:792–826.
12. Yucel YH, Zhang Q, Weinreb RN, Kaufman PL, Gupta N. Effects of retinal ganglion cell loss on magno-, parvo-, koniocellular pathways in the lateral geniculate nucleus and visual cortex in glaucoma. *Prog Retin Eye Res.* 2003;22:465–481.
13. Gupta N, Yucel YH. Glaucoma and the brain. *J Glaucoma.* 2001;10:S28–S29.
14. Graham SL, Klistorner AI, Goldberg I. Clinical application of objective perimetry using multifocal visual evoked potentials in glaucoma practice. *Arch Ophthalmol.* 2005;123:729–739.
15. Graham SL, Klistorner AI, Grigg JR, Billson FA. Objective VEP perimetry in glaucoma: asymmetry analysis to identify early deficits. *J Glaucoma.* 2000;9:10–19.
16. Hood DC, Thienprasiddhi P, Greenstein VC, et al. Detecting early to mild glaucomatous damage: a comparison of the multifocal VEP and automated perimetry. *Invest Ophthalmol Vis Sci.* 2004;45:492–498.
17. Parisi V, Miglior S, Manni G, Centofanti M, Bucci MG. Clinical ability of pattern electroretinograms and visual evoked potentials in detecting visual dysfunction in ocular hypertension and glaucoma. *Ophthalmology.* 2006;113:216–228.
18. Thienprasiddhi P, Greenstein VC, Chen CS, Liebmann JM, Ritch R, Hood DC. Multifocal visual evoked potential responses in glaucoma patients with unilateral hemifield defects. *Am J Ophthalmol.* 2003;136:34–40.
19. Thienprasiddhi P, Greenstein VC, Chu DH, et al. Detecting early functional damage in glaucoma suspect and ocular hypertensive patients with the multifocal VEP technique. *J Glaucoma.* 2006;15:321–327.
20. Kiyosawa M, Bosley TM, Kushner M, et al. Positron emission tomography to study the effect of eye closure and optic nerve damage on human cerebral glucose metabolism. *Am J Ophthalmol.* 1989;108:147–152.
21. Sugiyama T, Utsunomiya K, Ota H, Ogura Y, Narabayashi I, Ikeda T. Comparative study of cerebral blood flow in patients with normal-tension glaucoma and control subjects. *Am J Ophthalmol.* 2006;141:394–396.
22. Howseman AM, Bowtell RW. Functional magnetic resonance imaging: imaging techniques and contrast mechanisms. *Phil Trans R Soc Lond B Biol Sci.* 1999;354:1179–1194.
23. Turner R, Howseman A, Rees GE, Josephs O, Friston K. Functional magnetic resonance imaging of the human brain: data acquisition and analysis. *Exp Brain Res.* 1998;123:5–12.
24. Duncan RO, Sample PA, Weinreb RN, Bowd C, Zangwill LM. Retinotopic organization of primary visual cortex in glaucoma: a method for comparing cortical function with damage to the optic disk. *Invest Ophthalmol Vis Sci.* 2007;48:733–744.
25. Sunness JS, Liu T, Yantis S. Retinotopic mapping of the visual cortex using functional magnetic resonance imaging in a patient with central scotomas from atrophic macular degeneration. *Ophthalmology.* 2004;111:1595–1598.
26. Williams MA, Morris AP, McGlone F, Abbott DF, Mattingley JB. Amygdala responses to fearful and happy facial expressions under conditions of binocular suppression. *J Neurosci.* 2004;24:2898–2904.
27. Kerrigan-Baumrind LA, Quigley HA, Pease ME, Kerrigan DF, Mitchell RS. Number of ganglion cells in glaucoma eyes compared with threshold visual field tests in the same persons. *Invest Ophthalmol Vis Sci.* 2000;41:741–748.
28. Desatnik H, Quigley HA, Glovinsky Y. Study of central retinal ganglion cell loss in experimental glaucoma in monkey eyes. *J Glaucoma.* 1996;5:46–53.
29. Harwerth RS, Quigley HA. Visual field defects and retinal ganglion cell losses in patients with glaucoma. *Arch Ophthalmol.* 2006;124:853–859.
30. Crawford ML, Harwerth RS, Smith EL 3rd, Shen F, Carter-Dawson L. Glaucoma in primates: cytochrome oxidase reactivity in parvo- and magnocellular pathways. *Invest Ophthalmol Vis Sci.* 2000;41:1791–1802.
31. Crawford ML, Harwerth RS, Smith EL 3rd, Mills S, Ewing B. Experimental glaucoma in primates: changes in cytochrome oxidase blobs in V1 cortex. *Invest Ophthalmol Vis Sci.* 2001;42:358–364.
32. Chen E, Gedda U, Landau I. Thinning of the papillomacular bundle in the glaucomatous eye and its influence on the reference plane of the Heidelberg retinal tomography. *J Glaucoma.* 2001;10:386–389.
33. Guedes V, Schuman JS, Hertzmark E, et al. Optical coherence tomography measurement of macular and nerve fiber layer thickness in normal and glaucomatous human eyes. *Ophthalmology.* 2003;110:177–189.
34. Zeimer R, Asrani S, Zou S, Quigley H, Jampel H. Quantitative detection of glaucomatous damage at the posterior pole by retinal thickness mapping: a pilot study. *Ophthalmology.* 1998;105:224–231.
35. Harwerth RS, Carter-Dawson L, Shen F, Smith EL 3rd, Crawford ML. Ganglion cell losses underlying visual field defects from experimental glaucoma. *Invest Ophthalmol Vis Sci.* 1999;40:2242–2250.
36. Klistorner AI, Graham SL. Early magnocellular loss in glaucoma demonstrated using the pseudorandomly stimulated flash visual evoked potential. *J Glaucoma.* 1999;8:140–148.
37. Quigley HA, Sanchez RM, Dunkelberger GR, L'Hernault NL, Baginski TA. Chronic glaucoma selectively damages large optic nerve fibers. *Invest Ophthalmol Vis Sci.* 1987;28:913–920.
38. Glovinsky Y, Quigley HA, Dunkelberger GR. Retinal ganglion cell loss is size dependent in experimental glaucoma. *Invest Ophthalmol Vis Sci.* 1991;32:484–491.
39. King WM, Sarup V, Sauve Y, Moreland CM, Carpenter DO, Sharma SC. Expansion of visual receptive fields in experimental glaucoma. *Vis Neurosci.* 2006;23:137–142.
40. Sharma SC. Changes of central visual receptive fields in experimental glaucoma. *Prog Brain Res.* 2008;173:479–491.
41. Gupta N, Ly T, Zhang Q, Kaufman PL, Weinreb RN, Yucel YH. Chronic ocular hypertension induces dendrite pathology in the lateral geniculate nucleus of the brain. *Exp Eye Res.* 2007;84:176–184.
42. Gupta N, Yucel YH. Brain changes in glaucoma. *Eur J Ophthalmol.* 2003;13(suppl 3):S32–S35.

Downloaded from iovs.arvojournals.org on 01/17/2022

43. Lam DY, Kaufman PL, Gabelt BT, To EC, Matsubara JA. Neurochemical correlates of cortical plasticity after unilateral elevated intraocular pressure in a primate model of glaucoma. *Invest Ophthalmol Vis Sci.* 2003;44:2573–2581.
44. Eysel UT, Wolfhard U. The effects of partial retinal lesions on activity and size of cells in the dorsal lateral geniculate nucleus. *J Comp Neurol.* 1984;229:301–309.
45. Reinhard JF Jr, Liebmann JE, Schlosberg AJ, Moskowitz MA. Serotonin neurons project to small blood vessels in the brain. *Science.* 1979;206:85–87.
46. Vaucher E, Hamel E. Cholinergic basal forebrain neurons project to cortical microvessels in the rat: electron microscopic study with anterogradely transported Phaseolus vulgaris leucoagglutinin and choline acetyltransferase immunocytochemistry. *J Neurosci.* 1995; 15:7427–7441.
47. Yang G, Huard JM, Beitz AJ, Ross ME, Iadecola C. Stellate neurons mediate functional hyperemia in the cerebellar molecular layer. *J Neurosci.* 2000;20:6968–6973.
48. Gupta N, Ang LC, Noel de Tilly L, Bidaisee L, Yucel YH. Human glaucoma and neural degeneration in intracranial optic nerve, lateral geniculate nucleus, and visual cortex. *Br J Ophthalmol.* 2006;90:674–678.
49. Gupta N, Greenberg G, de Tilly LN, Gray B, Polemidiotis M, Yucel YH. Atrophy of the lateral geniculate nucleus in human glaucoma detected by magnetic resonance imaging. *Br J Ophthalmol.* 2009; 93:56–60.
50. Ito Y, Shimazawa M, Chen YN, et al. Morphological changes in the visual pathway induced by experimental glaucoma in Japanese monkeys. *Exp Eye Res.* 2009;89:246–255.
51. Sasaoka M, Nakamura K, Shimazawa M, Ito Y, Araie M, Hara H. Changes in visual fields and lateral geniculate nucleus in monkey laser-induced high intraocular pressure model. *Exp Eye Res.* 2008; 86:770–782.
52. Wang X, Sam-Wah Tay S, Ng YK. Nitric oxide, microglial activities and neuronal cell death in the lateral geniculate nucleus of glaucomatous rats. *Brain Res.* 2000;878:136–147.
53. Weber AJ, Chen H, Hubbard WC, Kaufman PL. Experimental glaucoma and cell size, density, and number in the primate lateral geniculate nucleus. *Invest Ophthalmol Vis Sci.* 2000;41:1370–1379.
54. Yucel YH, Zhang Q, Gupta N, Kaufman PL, Weinreb RN. Loss of neurons in magnocellular and parvocellular layers of the lateral geniculate nucleus in glaucoma. *Arch Ophthalmol.* 2000;118:378–384.
55. Yucel YH, Zhang Q, Weinreb RN, Kaufman PL, Gupta N. Atrophy of relay neurons in magno- and parvocellular layers in the lateral geniculate nucleus in experimental glaucoma. *Invest Ophthalmol Vis Sci.* 2001;42:3216–3222.
56. Gordon GR, Mulligan SJ, MacVicar BA. Astrocyte control of the cerebrovasculature. *Glia.* 2007;55:1214–1221.
57. Metea MR, Newman EA. Glial cells dilate and constrict blood vessels: a mechanism of neurovascular coupling. *J Neurosci.* 2006; 26:2862–2870.
58. Alkayed NJ, Birks EK, Narayanan J, Petrie KA, Kohler-Cabot AE, Harder DR. Role of P-450 arachidonic acid epoxygenase in the response of cerebral blood flow to glutamate in rats. *Stroke.* 1997;28:1066–1072.
59. Blanco VM, Stern JE, Filosa JA. Tone-dependent vascular responses to astrocyte-derived signals. *Am J Physiol.* 2008;294:H2855–H2863.
60. Zonta M, Angulo MC, Gobbo S, et al. Neuron-to-astrocyte signaling is central to the dynamic control of brain microcirculation. *Nat Neurosci.* 2003;6:43–50.
61. Ong K, Farinelli A, Billson F, Houang M, Stern M. Comparative study of brain magnetic resonance imaging findings in patients with low-tension glaucoma and control subjects. *Ophthalmology.* 1995;102:1632–1638.
62. Stroman GA, Stewart WC, Golnik KC, Cure JK, Olinger RE. Magnetic resonance imaging in patients with low-tension glaucoma. *Arch Ophthalmol.* 1995;113:168–172.
63. Harris A, Zarfati D, Zalish M, et al. Reduced cerebrovascular blood flow velocities and vasoreactivity in open-angle glaucoma. *Am J Ophthalmol.* 2003;135:144–147.
64. Harris A, Siesky B, Zarfati D, et al. Relationship of cerebral blood flow and central visual function in primary open-angle glaucoma. *J Glaucoma.* 2007;16:159–163.
65. Sheth SA, Nemoto M, Guiou M, et al. Columnar specificity of microvascular oxygenation and volume responses: implications for functional brain mapping. *J Neurosci.* 2004;24:634–641.
66. Duong TQ, Kim DS, Ugurbil K, Kim SG. Localized cerebral blood flow response at submillimeter columnar resolution. *Proc Natl Acad Sci U S A.* 2001;98:10904–10909.

Downloaded from iovs.arvojournals.org on 01/17/2022